Eur. Phys. J. A (2019) **55**: 159
DOI 10.1140/epja/i2019-12856-5

THE EUROPEAN PHYSICAL JOURNAL A

Regular Article – Experimental Physics

Longitudinal wobbling in ^{133}La

S. Biswas[1], R. Palit[1,a], S. Frauendorf[2], U. Garg[2], W. Li[2], G.H. Bhat[3,4], J.A. Sheikh[3,4], J. Sethi[1], S. Saha[1], Purnima Singh[1], D. Choudhury[1], J.T. Matta[2], A.D. Ayangeakaa[2], W.A. Dar[3], V. Singh[5], and S. Sihotra[5]

[1] Department of Nuclear and Atomic Physics, Tata Institute of Fundamental Research, Colaba, Mumbai, 400 005, India
[2] University of Notre Dame, Notre Dame, IN 46556, USA
[3] Department of Physics, University of Kashmir, Srinagar, 190 006, India
[4] Cluster University of Srinagar, Jammu and Kashmir, Srinagar, 190001, India
[5] Department of Physics, Panjab University, Chandigarh 160014, India

Received: 29 April 2019 / Revised: 7 July 2019
Published online: 20 September 2019

Communicated by C. Ur

Abstract. Excited states of ^{133}La have been investigated to search for the wobbling excitation mode in the low-spin regime. Wobbling bands with $n_\omega = 0$ and 1 are identified along with the interconnecting $\Delta I = 1$, $E2$ transitions, which are regarded as one of the characteristic features of wobbling motion. An increase in wobbling frequency with spin implies longitudinal wobbling for ^{133}La, in contrast with the case of transverse wobbling observed in ^{135}Pr. This is the first observation of a longitudinal wobbling band in nuclei. The experimental observations are accounted for by calculations using the quasiparticle-triaxial-rotor (QTR) model, which attribute the appearance of longitudinal wobbling to the early alignment of a $\pi = +$ proton pair.

The atomic nucleus is a fascinating mesoscopic system, which continues to reveal new collective excitation modes due to improved sensitivity in the experimental techniques [1–3]. For quadrupole deformed nuclei, loss of axial symmetry generates new types of collective excitations. The novel characteristic rotational features of triaxial nuclei are chirality and wobbling. The focus of the present communication is the wobbling mode, which emerges because a triaxial nucleus can carry collective angular momentum along all three principal axes. In contrast, an axial nucleus cannot rotate about its symmetry axis. The wobbling mode is well known for triaxial-rotor molecules [4]. It appears as a family of rotational bands based on excitations with increasing angular momentum components along the two axes with smaller moments of inertia. Its appearance in even-even triaxial nuclei was analyzed by Bohr and Mottelson [5]. It is characterized by an excitation energy, $E(I)$ $(= \hbar\omega)$ increasing with the angular momentum I and enhanced collective $\Delta I = 1$, $E2$ interconnecting transitions with reduced transition probabilities proportional to $1/I$.

The evidence for this mode in nuclei is rather limited. In a survey [6] across the nuclear chart using the finite-range liquid-drop model (FRLDM), soft triaxial ground-state shapes are predicted for nuclides around $Z = 62$, $N = 76$; $Z = 44$, $N = 64$; and $Z = 78$, $N = 116$. As reviewed in ref. [7], most of these nuclides seem to execute large-amplitude oscillations only around the axial shape. Partial evidence for stabilization of ground state triaxiality in these regions has been the observation of odd-I-low staggering of the quasi-γ band [8–11]. Reference [12] discussed the best case, ^{112}Ru: the quasi-γ band splits at high spin into the one- and two- phonon wobbling bands with the expected $\omega \propto I$. However, the data in ^{112}Ru [9] do not contain the required information about the $B(E2, I \to I-1)$ values to clearly establish the wobbling character.

More compelling evidence for the wobbling phenomenon was observed in the $A \sim 160$ mass region at high spin in the odd- A Lu and Ta isotopes [13–17] and at low spin in the $A \sim 130$ mass region in ^{135}Pr [18] as well as in the $A \sim 100$ mass region in ^{105}Pd [19]. The presence of the odd quasiparticle in these nuclei modifies the wobbling mode in a substantial way, which provides additional evidence for the triaxial shape. Frauendorf and Dönau have recently analyzed the modifications semiclassically [12]. They distinguish between two different kinds of wobbling modes for the odd-A nuclei. For the "longitudinal" mode, the angular momentum of the odd particle is parallel to the axis with the largest MoI, whereas for the "transverse" mode, it is perpendicular to this axis. The two modes can be recognized by the I-dependence of the

[a] e-mail: palit@tifr.res.in

wobbling energy $E_{wob}(I)$ $(= \hbar\omega_{wob})$, which increases or decreases, respectively. It is given by

$$E_{wob}(I) = E(I, n_\omega = 1) - [E(I-1, n_\omega = 0) + E(I+1, n_\omega = 0)]/2. \quad (1)$$

The wobbling bands observed in the Lu and Ta isotopes are examples of transverse wobbling because the wobbling frequency decreases with increasing spin, which also holds for the very recently reported first observation of transverse wobbling at low spin in ^{135}Pr [18]. The lowering of wobbling frequency enhances the detection probability and makes it possible to detect pattern of the enhanced reduced transition probabilities for interband $E2$ transitions, which is a crucial signal for wobbling. In all cases the high-j quasiproton has particle character. Its interaction with the triaxial core aligns its angular momentum with the short axis, and the medium axis has the maximal MoI, which results in *transverse* wobbling (see ref. [12]).

Here we report on observation of *longitudinal* wobbling in the nucleus ^{133}La, which is an isotone of ^{135}Pr. The $n_\omega = 1$ phonon band with band head at $13/2^-$, is found to decay to the $n_\omega = 0$ phonon band by $\Delta I = 1$, $E2$ transitions whose multipolarities have been determined on the basis of directional correlation from oriented states (DCO), polarization, and angular distribution measurements. The wobbling frequency is shown to increase with increasing spin indicating longitudinal wobbling. This is the first time that a longitudinal wobbling band has been observed in nuclei. Using the quasiparticle triaxial rotor (QTR) model with and without harmonic frozen approximation (HFA), the transition from transverse to longitudinal wobbling mode is demonstrated to be caused by the early alignment of a pair of positive-parity quasiprotons with the short axis.

A 52-MeV ^{11}B beam from the 14-UD Pelletron at Tata Institute of Fundamental Research (TIFR) was used to populate the excited states of ^{133}La via ^{126}Te(^{11}B, 4n) reaction. A layer of 1.1 mg/cm^2-thick enriched ^{126}Te evaporated on an Au backing of 9.9 mg/cm^2 served as the target. The emitted γ rays were detected in Indian National Gamma Array (INGA), which consisted of 21 Compton suppressed clover HPGe detectors coupled with a digital data acquisition system [20]. A set of 3×10^8 two- and higher-fold events were collected during the experiment. The time stamped data were sorted in a γ-γ-γ cube and angle dependent γ-γ matrices, and the RADWARE software package [21] was used for further analysis of these matrices and cubes.

A partial level scheme of ^{133}La containing the negative parity states studied in the present work, is shown in fig. 1. This level scheme is based on detailed analysis of the γ-γ-γ coincidence relations, cross-over transitions, and relative intensities of the concerned γ rays. Spin and parity assignments to the states have been made on the basis of the measured DCO ratios (R_{DCO}) and polarization asymmetries of the transitions depopulating these states. The detectors at 90° and 157° were used to determine the DCO ratios [22]. The polarization of γ rays was extracted from the 90° detectors using the formula given in refs. [23, 24].

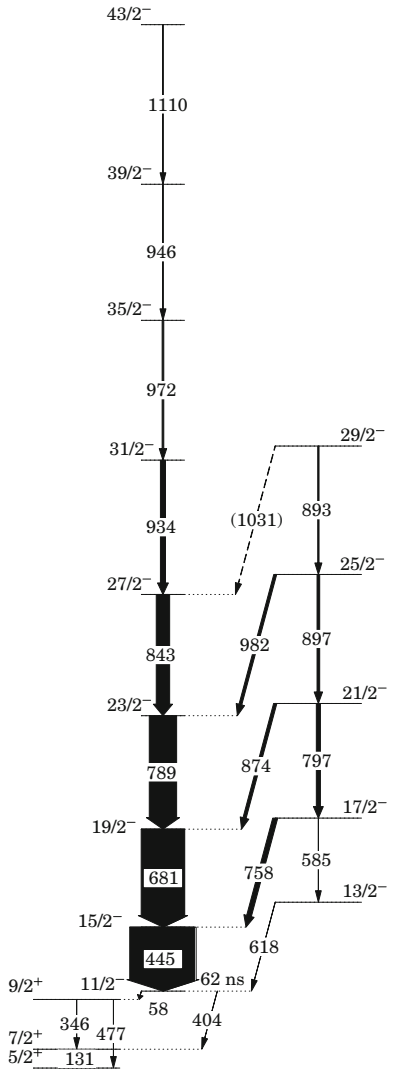

Fig. 1. Partial level scheme of ^{133}La showing the previously known yrast band ($n_\omega = 0$), and the $n_\omega = 1$ wobbling band. The intensities have been obtained from the 445-keV gated coincidence spectrum. The intensities of the transitions are proportional to the widths of the arrows.

Prior to the present work, the nucleus ^{133}La was studied through heavy-ion fusion evaporation reactions using a small detector array [25]. The present work confirms the previous results. More recently, a detailed level scheme of ^{133}La has been developed using ^{22}Ne + ^{116}Cd reaction and Gammasphere [26]. This elaborate level scheme showed presence of variety of exotic modes in ^{133}La at high spin such as triaxial bands, chirality and magnetic rotation [26]. Our study focuses on the measurement of mixing ratio of inter-band transitions at low spin which are essential for the investigation of wobbling mode in ^{133}La. Therefore, the present work aims to investigate the possible existence of a new wobbling mode in ^{133}La in addition to the exotic modes reported in the recent work [26]. The yrast and the yrare bands have been shown up to

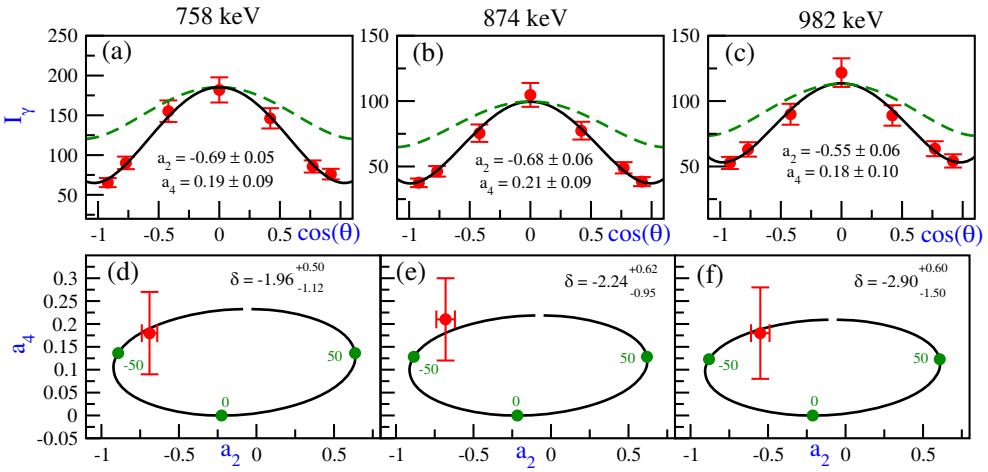

Fig. 2. (Color online) The angular distribution plots (the red points are the experimental points, the black solid curve shows the best fit to the data and the green dashed curve shows the curve for a pure $\Delta I = 1$, $M1$ transition) for (a) 758-keV, (b) 874-keV and (c) 982-keV transitions with a gate on 445-keV transition. The a_2-a_4 contour plots for (d) 758-keV, (e) 874-keV and (f) 982-keV transitions.

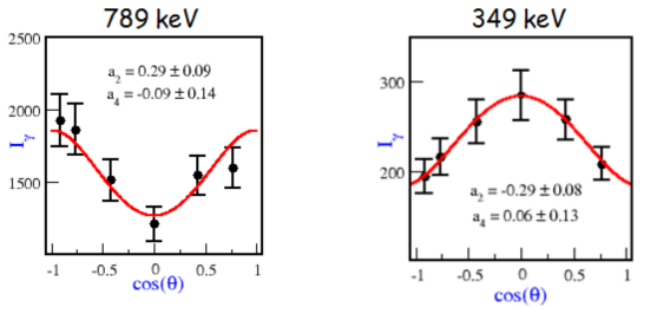

Fig. 3. (Color online) The angular distribution plots for the 789-keV $\Delta I = 2$ pure $E2$ transition and 349-keV $\Delta I = 1$ pure $M1$ transition present in ^{133}La. The 349-keV transition is not shown in fig. 1 and reported in refs. [25,26].

$I^\pi = 43/2^-$ and $I^\pi = 29/2^-$ in fig. 1 and identified as the $n_\omega = 0$ and $n_\omega = 1$ phonon wobbling bands, respectively. An important feature of the level scheme is the presence of connecting transitions from the $n_\omega = 1$ band to the yrast band.

One characteristic feature of wobbling bands is that the transitions between the $n_\omega = 1$ and $n_\omega = 0$ bands must be of $\Delta I = 1$, $E2$ character [13]. The angular distribution and DCO Ratio- Polarization methods have been used to extract the mixing ratio of the inter-band transitions. The angular distribution plots of 758, 874 and 982 keV inter-band transitions are depicted in figs. 2(a), (b) and (c), respectively. In figs. 2(d), (e) and (f), the $a_2 - a_4$ contour plots along with the experimental data points have been shown for these inter-band transitions. For comparison, the angular distribution plots of a pure $\Delta I = 2$ $E2$ and a pure $\Delta I = 1$ $M1$ transitions with energies 789 and 349 keV, respectively, are given in fig. 3. The spectra which have been used to extract the DCO ratio and polarization for the 758, 874 and 982-keV transitions are shown in figs. 4(a), (b), (c) and (d), (e), (f), respectively. The R_{DCO} and the polarization asymmetry for the 758 ($17/2^- \rightarrow 15/2^-$), 874 ($21/2^- \rightarrow 19/2^-$) and 982-keV ($25/2^- \rightarrow 23/2^-$) transitions were calculated as a function of mixing ratio (δ), which is the ratio of the reduced matrix elements for the $E2$ and $M1$ components of a parity non-changing $\Delta I = 1$ transition. The contour plot of theoretical R_{DCO} and polarization along with the experimental values are shown in fig. 4(g), (h) and (i). In the calculation of R_{DCO}, the width of the sub-state population (σ/I) was assumed to be 0.3. The mixing ratios obtained from both the DCO Ratio-Polarization and angular distribution methods have been shown in fig. 5 for the 758-, 874- and 982-keV connecting transitions. This comparison firmly confirms the $\Delta I = 1$, $E2$ nature of the inter-band transitions. However, the mixing ratios for the linking transitions mentioned in table 1 are from the DCO-Polarization method. The $E2$ fraction increases for the connecting transitions with increasing spin, indicating enhancement of wobbling with increasing angular momentum.

The experimental wobbling energies, E_{wob} (see eq. (1)) of the isotones ^{133}La and ^{135}Pr are plotted in fig. 6 as a function of spin. The wobbling frequency for ^{133}La is *increasing* with angular momentum, which along with the mixing ratios of the interconnecting transitions suggests longitudinal wobbling in ^{133}La [12], while it is *decreasing* in ^{135}Pr, for which transverse wobbling has been established [18]. The change from longitudinal to transverse in the neighboring isotones is a surprising result and warrants a detailed investigation. For both isotopes, the $h_{11/2}$ quasiproton has particle character, *i.e.*, it is expected to align with the short axis, which is confirmed by cranking calculations [25,27]. According to the general arguments of ref. [12], *both isotones should have been transverse.*

To identify the origin of this abrupt change from transverse to longitudinal wobbling motion, plots of the spin of the yrast band as function of the rotational frequency, $I(\omega)$, for the two nuclei are displayed in fig. 7. Both curves

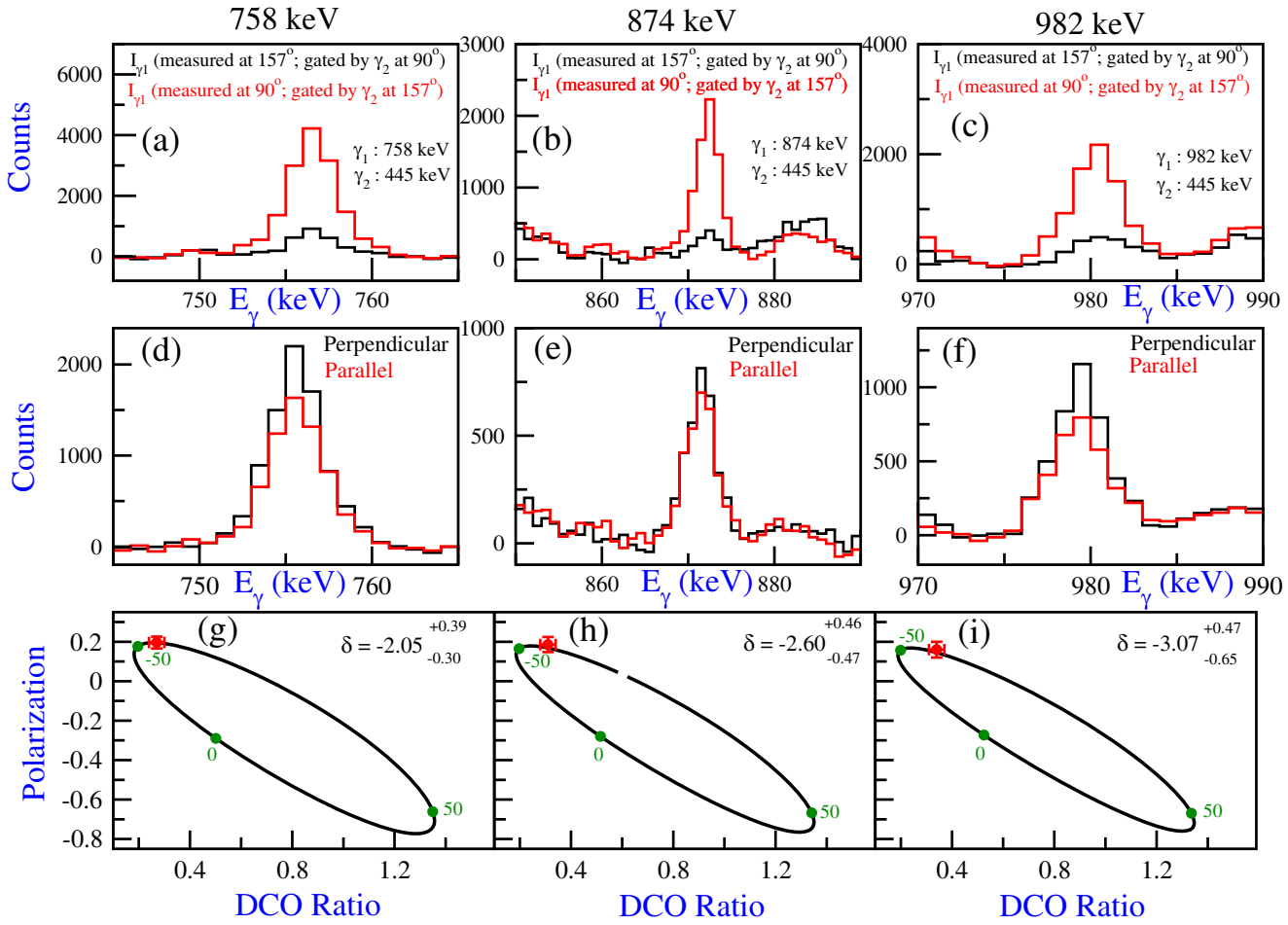

Fig. 4. (Color online) (a), (b) and (c) The spectra for the DCO Ratio, (d), (e) and (f) The perpendicular and parallel spectra for polarization, (g), (h) and (i) Contour plots for DCO Ratio *vs.* Polarization as a function of the mixing ratio (δ) (the red point on the ellipse is the experimental data point and the blue points represent the δ values) for 758-keV, 874-keV and 982-keV transitions, respectively, with a gate on 445-keV transition.

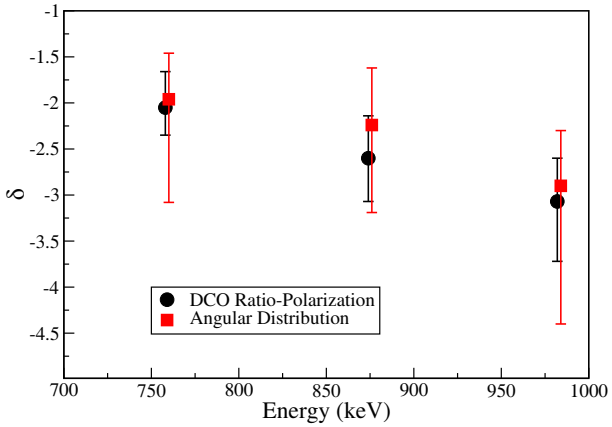

Fig. 5. (Color online) Comparison of mixing ratios extracted from DCO Ratio-Polarization method (black) and Angular Distribution Method (red) for 758, 874 and 982-keV transitions.

have an $\omega = 0$ intercept of about 5.5, which reflects the alignment of the $h_{11/2}$ proton with the short axis. The angular momentum increases early and in a gradual manner in ^{133}La compared to ^{135}Pr, which shows a late and rapid backbend. The change of the wobbling mode is, then, understood as follows. Just above the band head, both nuclides rotate about the short axis to which the $h_{11/2}$ proton is aligned. For ^{135}Pr, the MoI of the short axis is smaller than the MoI of the medium axis ($\mathcal{J}_s < \mathcal{J}_m$). With increasing spin it becomes favorable to put more and more collective angular momentum on the medium axis, which has the larger MoI. This leads to the decrease of the wobbling frequency with spin, the hallmark of transverse wobbling. As seen in fig. 7(a), the MoI of the short axis is larger for ^{133}La, such that the MoI of the two axes are about the same ($\mathcal{J}_s \sim \mathcal{J}_m$). The medium axis is no longer preferred by the collective angular momentum, which is now added to the short axis. This results in the increasing wobbling frequency with spin, which is the hallmark of longitudinal wobbling.

To quantify the claim, we modified the simple QTR+HFA model of ref. [12] by introducing a spin-dependent MoI for the short axis. We used the expression $\mathcal{J}_s = \Theta_0 + \Theta_1 R$, $R = I - i$, where $\mathcal{J}_s$ is MoI of the short axis, I is the total angular momentum, i the odd proton angular momentum, and R the core angular momentum. The experimental alignments shown in

Table 1. The mixing ratios (δ), $E2$ fractions ($= \delta^2/(1+\delta^2)$) and the experimental and theoretical transition probability ratios $\frac{B(M1_{out})}{B(E2_{in})}$ and $\frac{B(E2_{out})}{B(E2_{in})}$ using (quasiparticle triaxial rotor (QTR) model with and without harmonic frozen approximation (HFA)) for the transitions from the $n_\omega = 1$ to the $n_\omega = 0$ band in ^{133}La. Experimental ratios have been obtained from measured intensities of the transitions.

$I_i^\pi \to I_f^\pi$	E_γ	δ (expt.)	δ (QTR)	$E2$ fraction (%)	$\frac{B(M1_{out})}{B(E2_{in})}$ (expt.)	$\frac{B(M1_{out})}{B(E2_{in})}$ (QTR)	$\frac{B(E2_{out})}{B(E2_{in})}$ (expt.)	$\frac{B(E2_{out})}{B(E2_{in})}$ (QTR/HFA)
$13/2^- \to 11/2^-$	618	$-1.48^{+0.45}_{-0.32}$	-0.67	$68.6^{+13.1}_{-9.3}$	–	0.665	–	1.158/0.299
$17/2^- \to 15/2^-$	758	$-2.05^{+0.39}_{-0.30}$	-0.94	$80.8^{+5.9}_{-4.5}$	$0.107^{+0.035}_{-0.028}$	0.358	$1.127^{+0.140}_{-0.130}$	0.774/0.324
$21/2^- \to 19/2^-$	874	$-2.60^{+0.46}_{-0.47}$	-1.20	$87.1^{+4.0}_{-4.0}$	$0.056^{+0.018}_{-0.019}$	0.231	$0.716^{+0.079}_{-0.079}$	0.591/0.311
$25/2^- \to 23/2^-$	982	$-3.07^{+0.47}_{-0.65}$	-1.52	$90.4^{+2.6}_{-3.7}$	$0.039^{+0.011}_{-0.015}$	0.162	$0.545^{+0.057}_{-0.059}$	0.496/0.269
$29/2^- \to 27/2^-$	1031	–	-1.92	–	–	0.119	–	0.445 /0.221

fig. 8 are well accounted for with the parameters $\Theta_0 = 10, 13\,\hbar^2/\text{MeV}$, $\Theta_1 = 0.8, 0.2\,\hbar/\text{MeV}$, and $i = 4.5, 5\,\hbar$ for La and Pr, respectively. The other two MoI's were fixed at $\mathcal{J}_m = 21\,\hbar^2/\text{MeV}$ ($\mathcal{J}_m$ is MoI of the medium axis), and $\mathcal{J}_l = 4\,\hbar^2/\text{MeV}$ ($\mathcal{J}_l$ is MoI of the long axis) for both nuclides, as used in ref. [12]. As seen in fig. 6, the QTR+HFA calculation (depicted by HFA in the figure) reproduces the change from transverse wobbling in ^{135}Pr to longitudinal in ^{133}La. The reason is the early increase of the MoI in ^{133}La compared to ^{135}Pr seen in fig. 7. The ratios $\mathcal{J}_m/\mathcal{J}_s/\mathcal{J}_l$ for ^{135}Pr and ^{133}La at $I = 33/2$ are, respectively, 21/15.4/4 and 21/19/4, which correspond to transverse and longitudinal wobbling. The QTR+HFA values for $B(E2_{out})/B(E2_{in})$ also account for the data reasonably well (see table 1).

To further refine the theoretical interpretation we modified the QTR model used in ref. [12] in the same way as described for its HFA approximation. The core moments of inertia for ^{133}La were $\mathcal{J}_s = \Theta_0 + \Theta_1 R$ with $\Theta_0 = 12.5 \times 0.73\,\hbar^2/\text{MeV}$, $\Theta_1 = 0.9 \times 0.73\,\hbar/\text{MeV}$, $\mathcal{J}_m = 21 \times 0.73\,\hbar^2/\text{MeV}$, and $\mathcal{J}_l = 4 \times 0.73\,\hbar^2/\text{MeV}$. For ^{135}Pr they were $\mathcal{J}_s = \Theta_0 + \Theta_1 R$ with $\Theta_0 = 12.8\,\hbar^2/\text{MeV}$, $\Theta_1 = 0.14\,\hbar/\text{MeV}$, $\mathcal{J}_m = 21\,\hbar^2/\text{MeV}$, and $\mathcal{J}_l = 4\,\hbar^2/\text{MeV}$. A core-particle coupling strength of 6.4 was used, which corresponds to a deformation of $\varepsilon = 0.16$ and $\gamma = 26°$, which is the equilibrium deformation found in the TAC calculations and used for the triaxial rotor core.

The QTR also accounts for the change from transverse to longitudinal wobbling (see fig. 6) and the difference in alignment between the nuclei (see fig. 8). The QTR values for $B(M1)_{out}/B(E2)_{in}$, $B(E2)_{out}/B(E2)_{in}$, and the mixing ratios δ, also account for the data reasonably well (see table 1). The decrease of the ratio $B(M1)_{out}/B(E2)_{in}$ is reproduced as well; however QTR overestimates the ratio by factor of three. Importantly, the collective enhancement of the non-stretched $E2$ transitions from the wobbling to yrast band is born out by the QTR. The $E2$ fraction indicates that the transitions are $E2$ dominated. The negative sign of δ is consistent with the orientation of the $h_{11/2}$ quasiproton along the short axis.

We attribute the early increase of angular momentum in ^{133}La to the gradual alignment of a pair of positive-parity quasiprotons of (dg) nature with the short axis, which is at variance with previous interpretations [25,27]. Figure 7 shows that the positive-parity band based on the odd (dg) quasiproton does not show the early rise of angular momentum seen in the $h_{11/2}$ yrast band, because it is blocked by the odd proton. The curve displayed in the figure is shifted by $5.5\,\hbar$, the amount contributed by the aligned $h_{11/2}$. It crosses the yrast sequence about half-way the up-bend, which is expected when one quasiproton of the gradually aligning pair is excited. In the case of ^{135}Pr, the shifted curve of the positive parity (dg) keeps a relative distance of about $3\,\hbar$ to the yrast sequence until it runs into a backbend, caused by the alignment of other quasiparticles. The fact that its continuation crosses the yrast sequence may suggest that the alignment of a pair of (dg) quasiprotons participates in the backbend. It is noted that in ref. [26], the only interpretation of bands built on $11/2^-$ and $13/2^-$ in ^{133}La (identified as Q1 and Q2, respectively) is that they are based on $\pi h_{11/2}$. This is consistent with the longitudinal wobbling interpretation, which goes further by specifying that Q2 is the collective one-phonon wobbling excitation based on the $h_{11/2}$ quasiparticle state.

Additionally we carried out Tilted Axis Cranking calculations (TAC) [28] using the equilibrium deformation parameters $\varepsilon = 0.16$, $\gamma = 26°$ and the pair fields $\Delta_p = 0.7\,\text{MeV}$, $\Delta_n = 1.0\,\text{MeV}$. Rotation about the short axis turned out to be stable for the two signatures of the $h_{11/2}$ one-quasiproton configuration. The distance of the unfavored $\alpha = 1/2$ routhian to the favored $\alpha = -1/2$ routhian is included in fig. 6. The signature splitting is substantially larger for $Z = 57$ than $Z = 59$ because of the lower location in the $h_{11/2}$ shell. In case of ^{135}Pr, the TAC calculations place it somewhat higher than the wobbling band, which is consistent the experimental localization very close to it. In case of ^{133}La, TAC predicts it substantially higher, which explains the fact that we could not identify it in the present experiment.

In summary, the nature of the wobbling mode in ^{133}La has been investigated. Mixing ratios of interband transitions obtained from the angular distribution and DCO-polarization measurements indicate their strong $E2$ nature. Surprisingly, ^{133}La shows longitudinal wobbling as the wobbling frequency is increasing with spin. This is the first observation of *longitudinal* wobbling band in nuclei. The quasiparticle plus triaxial rotor model (with and

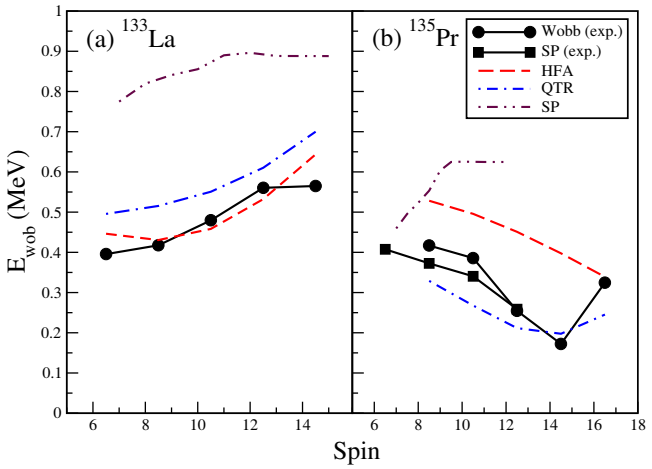

Fig. 6. (Color online) Comparison between experiment (solid lines) and theory (HFA (dashed lines), QTR (dash-dotted lines)) of the variation of wobbling frequency for $n_\omega = 1$ band in (a) ^{133}La and (b) ^{135}Pr. The dash-dot-dot line denoted by SP shows the position of the unfavored proton $h_{11/2}$ signature partner relative to the favored yrast sequence, as calculated by the Tilted Axis Cranking (TAC) model.

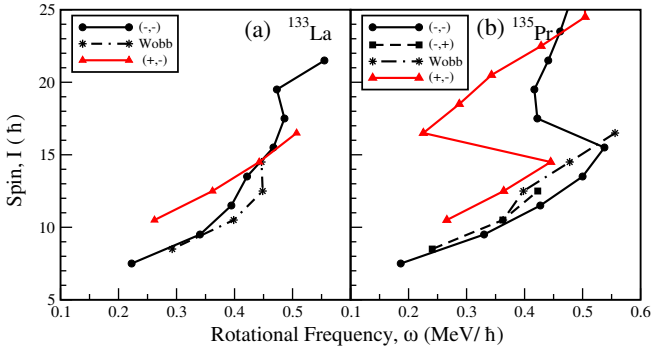

Fig. 7. (Color online) Spin (I) *vs.* experimental rotational frequency (ω) for (a) ^{133}La and (b) ^{135}Pr. Shown in black are the $h_{11/2}$ favored signature sequence (full circle), its unfavored signature partner (dash with square), and the wobbling band (dash-dot with star). The full red curve (triangles) shows the positive-parity sequence $(\pi, \alpha) = (+, -1/2)$ shifted up by 5.5.

without harmonic frozen approximation), was able to reproduce the experimental energies and transition rates, and clearly point to a transition from transverse wobbling in ^{135}Pr to longitudinal wobbling in ^{133}La. The change from transverse wobbling to longitudinal wobbling is understood as follows: In ^{135}Pr only the $h_{11/2}$ quasiproton is aligned with the short axis of the triaxial density distribution and the medium axis has the largest MoI. This arrangement gives transverse wobbling. In ^{133}La an additional pair of positive parity (dg) quasiprotons aligns early and gradually with the short axis. The additional alignment increases the effective MoI of the short axis, which becomes larger than the MoI of the medium axis. This arrangement gives longitudinal wobbling. In ^{135}Pr the early (dg) neutron alignment occurs later as part of the sharp band crossing, above which the longitudinal wobbling begins to appear [18].

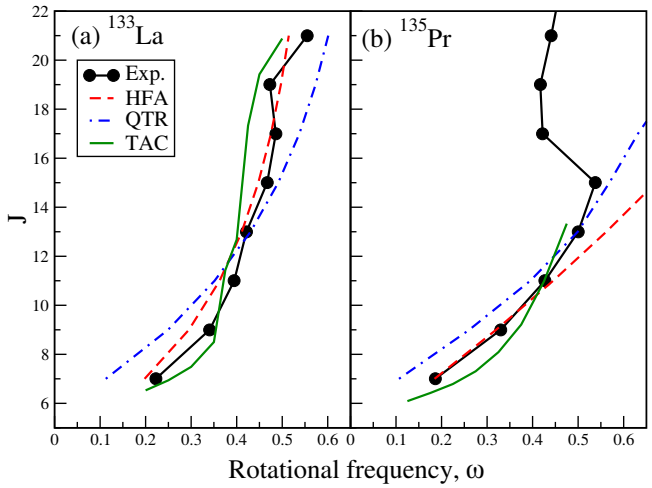

Fig. 8. (Color online) ($J = I - 1/2$) *vs.* experimental (black circle) rotational frequency (ω) for the $h_{11/2}$ favored signature sequence in (a) ^{133}La and (b) ^{135}Pr compared with HFA (dash Red), QTR (dash-dot Blue), and TAC (full green) calculations.

We acknowledge the TIFR-BARC Pelletron Linac Facility for providing good quality beam. The help and cooperation of the INGA collaboration in setting up the array is also acknowledged. We thank the TIFR central workshop for the fabrication of various mechanical components for the experiment. This work has been supported in part by the Department of Science and Technology, Government of India (No. IR/S2/PF-03/2003-II), the U.S. National Foundation (Grant No. PHY-1419765), and the US Department of Energy (Grant DE-FG02-95ER40934).

Data Availability Statement This manuscript has no associated data or the data will not be deposited. [Authors' comment: All data generated during this study are contained in this published article.]

Publisher's Note The EPJ Publishers remain neutral with regard to jurisdictional claims in published maps and institutional affiliations.

References

1. R.M. Clark *et al.*, Phys. Rev. Lett. **78**, 1868 (1997).
2. D.R. Jensen *et al.*, Phys. Rev. Lett. **89**, 142503 (2002).
3. H. Iwasaki *et al.*, Phys. Rev. Lett. **112**, 142502 (2014).
4. G. Herzberg, *Molecular Spectra and Molecular Structure*, Vol. **2**, *Infraread and Raman Spectra of Polyatomic Molecules*, 2nd edition (van Nostrand, New York, 1950).
5. A. Bohr, B. Mottelson, *Nuclear Structure*, Vol. **II** (Benjamin, Inc., New York, 1975).
6. Peter Möller, Ragnar Bengtsson, B.G. Carlsson, Peter Olivius, Takatoshi Ichikawa, Phys. Rev. Lett. **97**, 162502 (2006).
7. S. Frauendorf, Int. J. Mod. Phys. E **24**, 1541001 (2015).

8. I. Stefanescu *et al.*, Nucl. Phys. A **789**, 125 (2007).
9. S.J. Zhu *et al.*, Int. J. Mod. Phys. E **18**, 1717 (2009).
10. Y.X. Luo *et al.*, Nucl. Phys. A **919**, 67 (2013).
11. Y. Toh *et al.*, Phys. Rev. C **87**, 041304(R) (2013).
12. S. Frauendorf, F. Dönau, Phys. Rev. C **89**, 014322 (2014).
13. S.W. Ødegård *et al.*, Phys. Rev. Lett. **86**, 5866 (2001).
14. G. Schönwaßer *et al.*, Phys. Lett. B **552**, 9 (2003).
15. H. Amro *et al.*, Phys. Lett. B **553**, 197 (2003).
16. P. Bringel *et al.*, Eur. Phys. J. A **24**, 167 (2005).
17. D.J. Hartley *et al.*, Phys. Rev. C **80**, 041304(R) (2009).
18. J.T. Matta *et al.*, Phys. Rev. Lett. **114**, 082501 (2015).
19. J. Timár *et al.*, Phys. Rev. Lett. **122**, 062501 (2019).
20. R. Palit *et al.*, Nucl. Instrum. Methods Phys. Res. Sect. A **680**, 90 (2012).
21. D.C. Radford, Nucl. Instrum. Methods Phys. Res. Sect. A **361**, 297 (1995).
22. A. Krämer-Flecken, T. Morek, R.M. Leider, W. Gast, G. Hebbinghaus, H.M. Jäger, W. Urban, Nucl. Instrum. Methods Phys. Res. Sect. A **275**, 333 (1989).
23. K. Starosta *et al.*, Nucl. Instrum. Methods Phys. Res. Sect. A **423**, 16 (1999).
24. R. Palit, H.C. Jain, P.K. Joshi, S. Nagaraj, B.V.T. Rao, S.N. Chintalapudi, S.S. Ghugre, Pramana **54**, 347 (2000).
25. L. Hildingson, W. Klamra, Th. Lindblad, C.G. Lindén, G. Sletten, G. Székely, Z. Phys. A **338**, 125 (1991).
26. C.M. Petrache *et al.*, Phys. Rev. C **94**, 064309 (2016).
27. T.M. Semkov *et al.*, Phys. Rev. C **34**, 523 (1986).
28. S. Frauendorf, Nucl. Phys. A **677**, 115 (2000).